

Self-Similar Solutions in the Homogeneous Isotropic Turbulence

Nicola de Divitiis*

Department of Mechanics and Aeronautics

University "La Sapienza", Rome, Italy

(Dated: November 4, 2018)

Abstract

We calculate the self-similar longitudinal velocity correlation function, the energy spectrum and the corresponding other properties using the results of the Lyapunov analysis of the isotropic homogeneous turbulence just presented by the author in a previous work [1]. The correlation functions correspond to steady-state solutions of the evolution equation under the self-similarity hypothesis introduced by von Kármán. These solutions are numerically calculated and the results adequately describe several properties of the isotropic turbulence.

PACS numbers: Valid PACS appear here

arXiv:0904.0818v2 [physics.flu-dyn] 20 Jun 2009

*via Eudossiana, 18, 00184, Rome; Electronic address: dedivitiis@dma.dma.uniroma1.it

I. ANALYSIS

A recent work of the author, which deals with the Lyapunov analysis of the isotropic turbulence [1], suggests a mechanism for the transferring of the kinetic energy between the length scales which is based on the Landau hypothesis about the bifurcations of the fluid kinematic equations [2]. The analysis expresses the velocity fluctuation through the Lyapunov theory and leads to the closure of the von Kármán-Howarth equation which gives the longitudinal velocity correlation function for two points [3], i.e.

$$\frac{\partial f}{\partial t} = \frac{K(r)}{u^2} + 2\nu \left(\frac{\partial^2 f}{\partial r^2} + \frac{4}{r} \frac{\partial f}{\partial r} \right) - 10\nu f \frac{\partial^2 f}{\partial r^2}(0) \quad (1)$$

where $K(r)$, related to the triple velocity correlation function, realizes the closure of the Eq. (1) through the following relation [1]

$$K = u^3 \sqrt{\frac{1-f}{2}} \frac{\partial f}{\partial r} \quad (2)$$

and u is the standard deviation of the longitudinal velocity u_r , which satisfies [3, 4]

$$\frac{du^2}{dt} = 10\nu u^2 \frac{\partial^2 f}{\partial r^2}(0) \quad (3)$$

The skewness of Δu_r can be expressed as [4]

$$H_3(r) = \frac{\langle (\Delta u_r)^3 \rangle}{\langle (\Delta u_r)^2 \rangle^{3/2}} = \frac{6k(r)}{(2(1-f(r)))^{3/2}} \quad (4)$$

where, $k(r)$ is the longitudinal triple velocity correlation function, related to $K(r)$ through [4]

$$K(r) = u^3 \left(\frac{\partial}{\partial r} + \frac{4}{r} \right) k(r) \quad (5)$$

As the result, the skewness of $\partial u_r / \partial r$ is a constant which does not depend on the Reynolds number, whose value is $H_3(0) = -3/7$ [1]. The other dimensionless statistical moments are consequently determined, taking into account that the longitudinal velocity difference can be expressed as [1]

$$\frac{\Delta u_r}{\sqrt{\langle (\Delta u_r)^2 \rangle}} = \frac{\xi + \psi (\chi(\eta^2 - 1) - (\zeta^2 - 1))}{\sqrt{1 + 2\psi^2 (1 + \chi^2)}} \quad (6)$$

Equation (6) arises from statistical considerations about the Navier-Stokes equations and expresses the internal structure of the isotropic turbulence, where ξ , η and ζ are independent

centered random variables which exhibit the gaussian distribution functions $p(\xi)$, $p(\eta)$ and $p(\zeta)$ whose standard deviation is equal to the unity, and ψ is [1]

$$\psi(\mathbf{r}, R) = \sqrt{\frac{R}{15\sqrt{15}}} \hat{\psi}(\mathbf{r}, R) \quad (7)$$

The quantity $R = u\lambda_T/\nu$ is the Taylor-scale Reynolds number, where $\lambda_T = u/\sqrt{\langle(\partial u_r/\partial r)^2\rangle}$ is the Taylor-scale, whereas the function $\hat{\psi}(\mathbf{r}, R)$ is determined as $H_3(r)$ is known. The parameter χ is also a function of R which is given by [1]

$$\frac{8\psi_0^3(1-\chi^3)}{(1+2\psi_0^2(1+\chi^2))^{3/2}} = \frac{3}{7} \quad (8)$$

with $\psi_0 = \psi(R, 0)$ and $\hat{\psi}_0 = 1.075$ [1]. From Eqs. (6) and (7), all the absolute values of the dimensionless moments of Δu_r of order greater than 3 rise with R , indicating that the intermittency increases with the Reynolds number.

The PDF of Δu_r can be formally expressed with the Frobenius-Perron equation

$$F(\Delta u'_r) = \int_{\xi} \int_{\eta} \int_{\zeta} p(\xi)p(\eta)p(\zeta) \delta(\Delta u_r - \Delta u'_r) d\xi d\eta d\zeta \quad (9)$$

where δ is the Dirac delta, whereas the spectrums $E(\kappa)$ and $T(\kappa)$ are calculated as the Fourier Transforms of f and K [4], respectively, i.e.

$$\begin{bmatrix} E(\kappa) \\ T(\kappa) \end{bmatrix} = \frac{1}{\pi} \int_0^{\infty} \begin{bmatrix} u^2 f(r) \\ K(r) \end{bmatrix} \kappa^2 r^2 \left(\frac{\sin \kappa r}{\kappa r} - \cos \kappa r \right) dr \quad (10)$$

II. SELF-SIMILARITY

In this section the properties of the self-similar solutions of the von Kármán-Howarth equation are studied.

Far from the initial condition, it is reasonable that the mechanism of the cascade of energy and the effects of the viscosity act keeping f and $E(\kappa)$ similar in the time. This is the idea of self-preserving correlation function and turbulence spectrum which was originally introduced by von Kármán (see ref. [5] and reference therein).

In order to analyse this self-similarity, it is convenient to express f in terms of the dimensionless variables $\hat{r} = r/\lambda_T$ and $\hat{t} = tu/\lambda_T$, i.e., $f = f(\hat{t}, \hat{r})$. As the result, Eq. (1) reads as follows

$$\frac{\partial f}{\partial \hat{t}} \frac{\lambda_T}{u} \frac{d}{dt} \left(\frac{tu}{\lambda_T} \right) - \frac{\partial f}{\partial \hat{r}} \frac{\hat{r}}{u} \frac{d\lambda_T}{dt} = \sqrt{\frac{1-f}{2}} \frac{\partial f}{\partial \hat{r}} + \frac{2}{R} \left(\frac{\partial^2 f}{\partial \hat{r}^2} + \frac{4}{\hat{r}} \frac{\partial f}{\partial \hat{r}} \right) + \frac{10}{R} f \quad (11)$$

where $\partial^2 f / \partial \hat{r}^2(0) \equiv -1$. This is a non-linear partial differential equation whose coefficients vary in time according to the rate of kinetic energy

$$\frac{du^2}{dt} = -\frac{10\nu u^2}{\lambda_T^2} \quad (12)$$

If the self-similarity is assumed, all the coefficients of Eq. (11) must not vary with the time [3, 5], thus one obtains

$$R = \text{const} \quad (13)$$

$$a_1 \equiv \frac{\lambda_T}{u} \frac{d}{dt} \left(\frac{tu}{\lambda_T} \right) = \text{const} \quad (14)$$

$$a_2 \equiv \frac{1}{u} \frac{d\lambda_T}{dt} = \text{const}, \quad (15)$$

As the consequence of Eqs. (12) and (13), λ_T and u will depend upon the time according to

$$\lambda_T(t) = \lambda_T(0) \sqrt{1 + 10\nu/\lambda_T^2(0)t}, \quad u(t) = \frac{u(0)}{\sqrt{1 + 10\nu/\lambda_T^2(0)t}}. \quad (16)$$

From these expressions, the corresponding values of a_1 and a_2 are

$$a_1 \equiv \frac{\lambda_T}{u} \frac{d}{dt} \left(\frac{tu}{\lambda_T} \right) = \frac{1}{1 + 10\nu t / \lambda_T^2}, \quad (17)$$

$$a_2 \equiv \frac{1}{u} \frac{d\lambda_T}{dt} = \frac{5}{R}$$

The coefficient a_1 decreases with the time and for $t \rightarrow \infty$, $a_1 \rightarrow 0$, whereas a_2 remains constant. Therefore, for $t \rightarrow \infty$, one obtains the self-similar correlation function $f(\hat{r})$, which does not depend on the initial condition and that obeys to the following non-linear ordinary differential equation

$$\frac{5}{R} \frac{df}{d\hat{r}} \hat{r} + \sqrt{\frac{1-f}{2}} \frac{df}{d\hat{r}} + \frac{2}{R} \left(\frac{d^2 f}{d\hat{r}^2} + \frac{4}{\hat{r}} \frac{df}{d\hat{r}} \right) + \frac{10}{R} f = 0 \quad (18)$$

The first term of Eq. (18) represents the variations in time of f which does not influence the mechanism of energy cascade. This term is negligible with respect to the second one only if $\hat{r} \ll R$, and is responsible for the asymptotic behavior of f which is expressed by $f \approx 1/\hat{r}^2$. This behavior determines that all the integral scales of f diverge and that f does not admit Fourier transform, thus the corresponding energy spectrum is not defined. According to von Kármán [3, 5], we search the self-similar solutions over the whole range of \hat{r} , with the exception of the dimensionless distances whose order magnitude exceed R . This corresponds to assume the self-similarity for all the frequencies of the energy spectrum, but for the lowest ones [3, 5]. As the result, the first term of Eq. (18) can be neglected with respect to the second one, and the equation for f reads as follows

$$\sqrt{\frac{1-f}{2}} \frac{df}{d\hat{r}} + \frac{2}{R} \left(\frac{d^2f}{d\hat{r}^2} + \frac{4}{\hat{r}} \frac{df}{d\hat{r}} \right) + \frac{10}{R} f = 0 \quad (19)$$

The analysis of Eq. (19) shows that $f \simeq 1 - \hat{r}^2/2 + (10 + R)/112 \hat{r}^4$ in the vicinity of the origin and that $f - 1 \approx \hat{r}^{2/3}$ when the first term of Eq. (19) is about constant, whereas for large \hat{r} , f exponentially decreases. Thus, all the integral scales of f are finite quantities and the energy spectrum is a definite quantity whose integral over the Fourier space gives the turbulent kinetic energy.

III. RESULTS AND DISCUSSION

In this section we calculate the solutions of Eq. (19) and study the corresponding properties of the self-similar solutions. To determine f and its energy spectrum, consider the following initial condition problem with respect to the dimensionless separation distance \hat{r}

$$\begin{aligned} \frac{df}{d\hat{r}} &= F \\ \frac{dF}{d\hat{r}} &= -5f - \left(\frac{1}{2} \sqrt{\frac{1-f}{2}} R + \frac{4}{\hat{r}} \right) F \end{aligned} \quad (20)$$

This ordinary differential system arises from Eq. (19) and its initial condition is $f(0) = 1$, $F(0) = 0$.

Several numerical solutions of Eqs. (20) were calculated for different Taylor scale Reynolds numbers by means of the fourth-order Runge-Kutta scheme of integration. The cases here

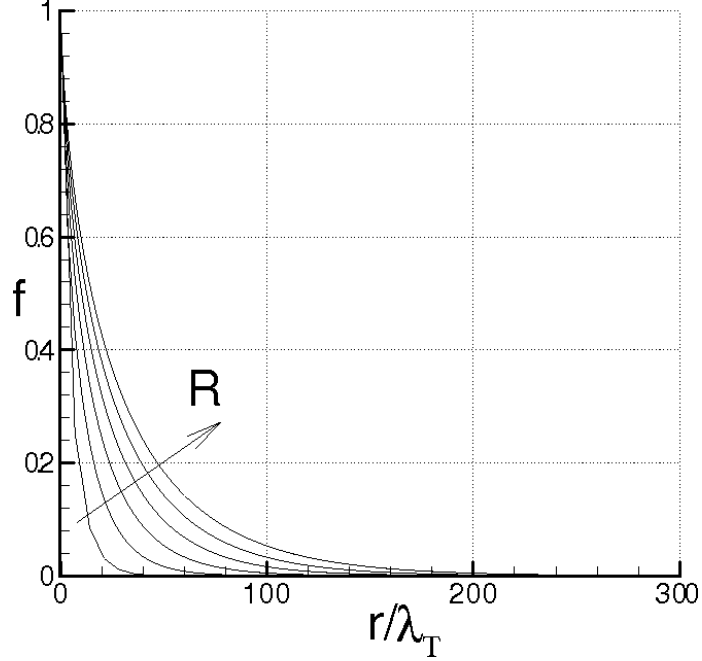


FIG. 1: Longitudinal correlation function for different Taylor-Scale Reynolds numbers.

analyzed correspond to $R=100, 200, 300, 400, 500$ and 600 . The fixed step size of the integrator scheme is selected on the basis of the asymptotic stability condition $\Delta\hat{r} = \sqrt{2}/R$ [6], which also provides a fairly accurate description of the energy spectrum at the large

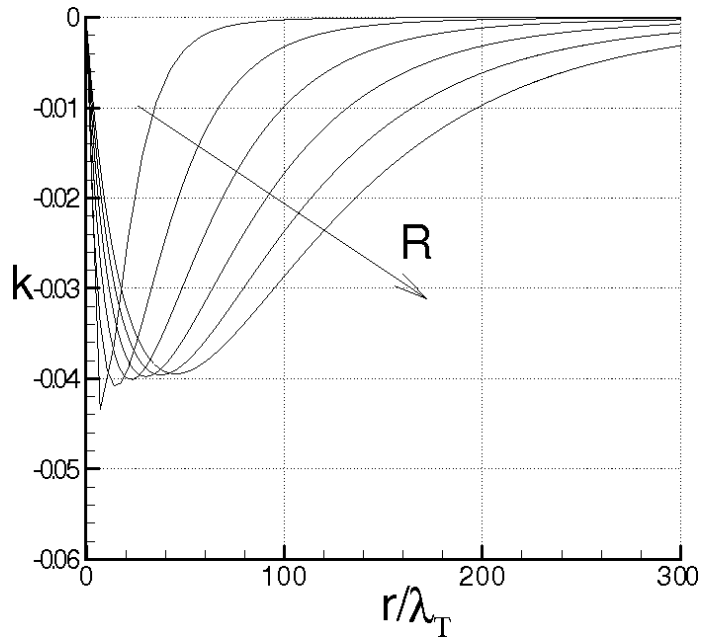


FIG. 2: Longitudinal triple correlation function for different Taylor-Scale Reynolds numbers.

wave-numbers.

Figures 1 and 2 show the numerical solutions of Eqs. (20), where double and triple longitudinal correlation functions are represented in terms of \hat{r} , for the different values of R . Due to the mechanism of energy cascade, the tail of f rises with R and the maximum of $|k|$ gives the entity of this mechanism. This value is slightly less than 0.05 and agrees quite well with the numerous data of the literature which concern the evolution of the correlation functions. It is apparent that the spatial variations of k correspond to dimensionless scales \hat{r} whose size increases with R .

Figures 3 and 4 show the plots of $E(\kappa)$ and $T(\kappa)$ for the same Reynolds numbers. As the consequence of the mathematical properties of f , the energy spectrum behaves like $E(\kappa) = O(\kappa^4)$ in proximity of the origin, and after a maximum is about parallel to the $-5/3$ Kolmogorov law (dashed line in Fig. 3) in a given interval of the wave-numbers. This interval defines the inertial range of Kolmogorov, and its size increases with R . For higher wave-numbers the energy spectrum rapidly decreases with a slope which depends on the behavior of f in proximity of the origin and thus on the Reynolds number.

Since K does not modify the kinetic energy of the flow, according to Eq. (2), the integral of $T(\kappa)$ over the Fourier wave-numbers results to be identically equal to zero at all the Reynolds numbers.

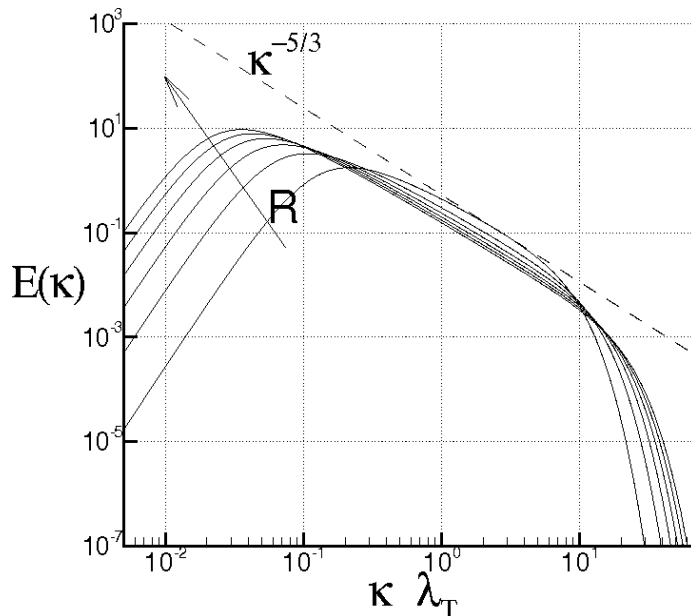


FIG. 3: Turbulent Energy Spectrum for different Taylor-Scale Reynolds numbers.

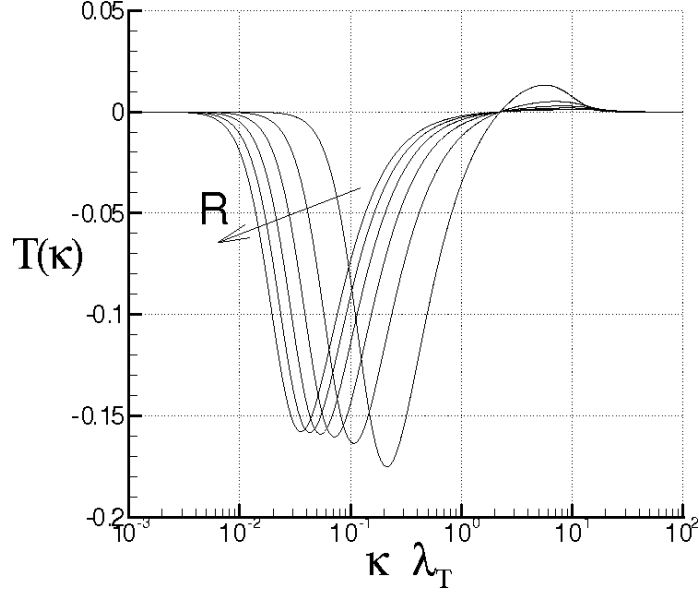


FIG. 4: "Transfer function $T(\kappa)$ " for several Taylor-Scale Reynolds numbers.

In the Figs. 5 and 6, skewness and flatness of Δu_r are shown in terms of \hat{r} for the same values of R . The skewness H_3 is first calculated according to Eq. (4) and thereafter the flatness H_4 has been determined using Eq. (6). For a given R , $|H_3|$ starts from $3/7$ at the origin, then decreases to small values, while H_4 starts from values quite greater than 3 at $r = 0$, then reaches the value of 3 (faster than H_3 tending to zero). Although $H_3(0)$ does

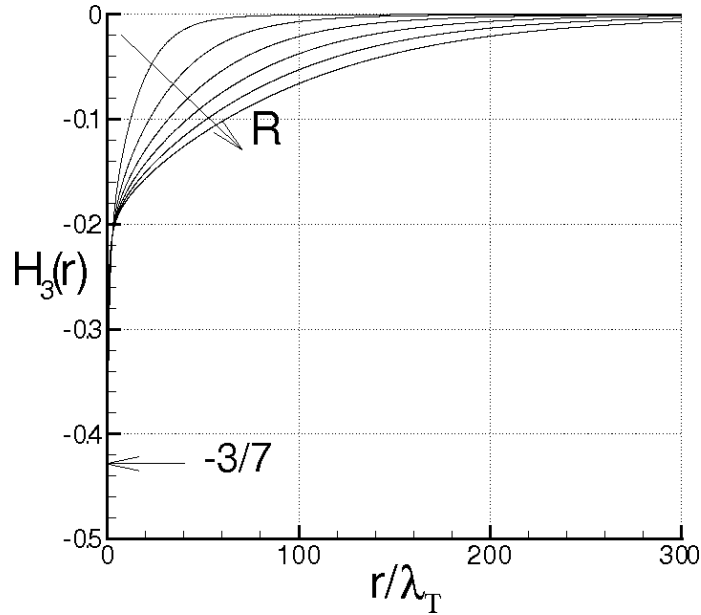


FIG. 5: Skewness of Δu_r at different Taylor-Scale Reynolds numbers.

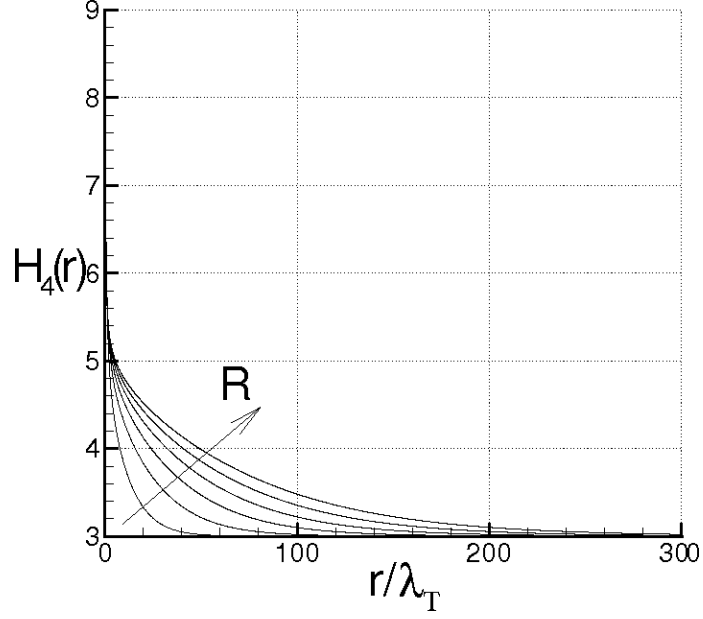


FIG. 6: Flatness of Δu_r at different Taylor-Scale Reynolds numbers.

not depend upon R , $H_3(\hat{r})$ is a rising function of R and, in any case, the intermittency of Δu_r increases with R according to Eqs. (6) and (7).

Next, the Kolmogorov function $Q(r)$ and Kolmogorov constant C , are determined using

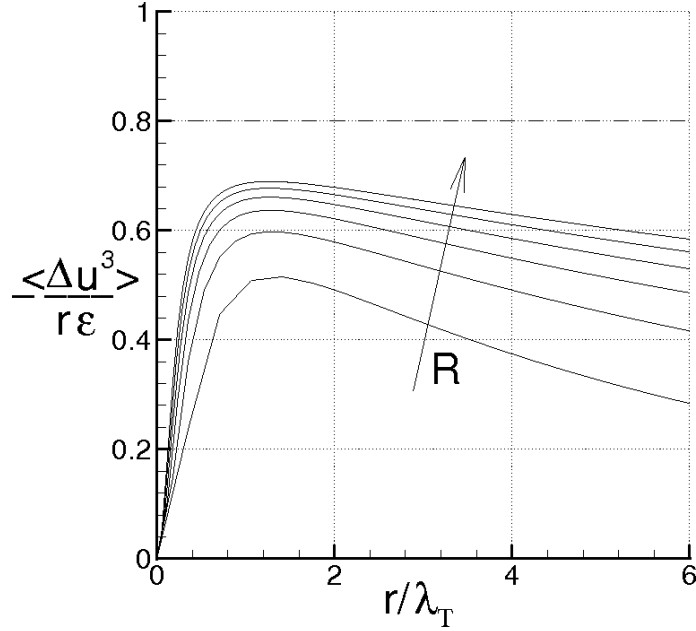


FIG. 7: Kolmogorov function for several Taylor-Scale Reynolds numbers.

| R | C |
|-----|--------|
| 100 | 1.8860 |
| 200 | 1.9451 |
| 300 | 1.9704 |
| 400 | 1.9847 |
| 500 | 1.9940 |
| 600 | 2.0005 |

TABLE I: Kolmogorov constant for different Taylor-Scale Reynolds number.

the previous results. According to the theory, the Kolmogorov function, defined as

$$Q(r) = -\frac{\langle(\Delta u_r)^3\rangle}{r\varepsilon} \quad (21)$$

is constant with respect to r , and is equal to $4/5$ as long as $r/\lambda_T = O(1)$. As shown in Fig. 7, $Q(r)$ exhibits a maximum for $\hat{r} = O(1)$ and quite small variations for higher \hat{r} , as the Reynolds number increases. This maximum increases with R , and seems to tend toward the limit $4/5$ prescribed by the Kolmogorov theory.

The Kolmogorov constant C , defined by $E(\kappa) \approx C\varepsilon^{2/3}/\kappa^{5/3}$, is here calculated as

$$C = \max_{\kappa \in (0, \infty)} \frac{E(\kappa)\kappa^{5/3}}{\varepsilon^{2/3}} \quad (22)$$

where $\varepsilon = -3/2 du^2/dt$ is the rate of the energy of dissipation. In the table I, the Kolmogorov constant is reported in terms of the Taylor-scale Reynolds number. The obtained values of C and Q_{max} are in good agreement with the corresponding values known from the various literature.

The spatial structure of Δu_r , expressed by Eq. (6), is also studied with the previous results.

According to the various works [8, 9, 10], Δu_r behaves quite similarly to a multifractal system, where Δu_r obeys to a law of the kind $\Delta u_r(r) \approx r^q$ in which q is a fluctuating exponent. This implies that the statistical moments of $\Delta u_r(r)$ are expressed through different scaling exponents $\zeta(n)$ whose values depend on the moment order n , i.e.

$$\langle(\Delta u_r)^n(r)\rangle = Ar^{\zeta(n)} \quad (23)$$

In order to calculate these exponents, the statistical moments of Δu_r are first calculated

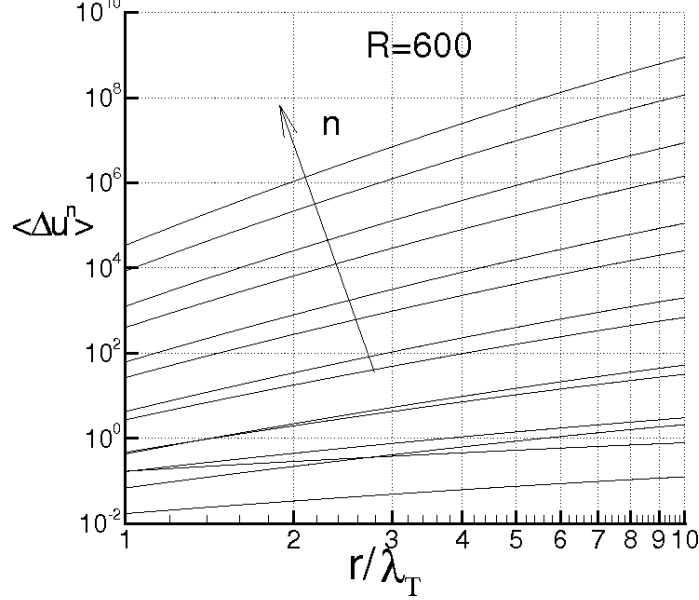


FIG. 8: Statistical moments of Δu_r in terms of the separation distance, for $R=600$.

using Eqs. (6) and (9) for several separation distances. Figure 8 shows the evolution of the statistical moments of Δu_r in terms of \hat{r} , in the case of $R = 600$. The scaling exponents of Eq. (23) are identified through a best fitting procedure, in the intervals (\hat{r}_1, \hat{r}_2) , where the endpoints \hat{r}_1 and \hat{r}_2 have to be determined. The calculation of $\zeta(n)$ and A_n is carried out through a minimum square method which, for each moment order, is applied to the following optimization problem

$$J_n(\zeta(n), A_n) \equiv \int_{\hat{r}_1}^{\hat{r}_2} (\langle (\Delta u_r)^n \rangle - A_n r^{\zeta(n)})^2 dr = \min, \quad n = 1, 2, \dots \quad (24)$$

| R | $\zeta(1)$ | $\zeta(2)$ | $\zeta(3)$ | $\zeta(4)$ | $\zeta(5)$ | $\zeta(6)$ | $\zeta(7)$ | $\zeta(8)$ | $\zeta(9)$ | $\zeta(10)$ | $\zeta(11)$ | $\zeta(12)$ | $\zeta(13)$ | $\zeta(14)$ | $\zeta(15)$ |
|-----|------------|------------|------------|------------|------------|------------|------------|------------|------------|-------------|-------------|-------------|-------------|-------------|-------------|
| 100 | 0.35 | 0.70 | 1.00 | 1.30 | 1.56 | 1.82 | 2.06 | 2.31 | 2.53 | 2.76 | 2.97 | 3.18 | 3.39 | 3.59 | 3.79 |
| 200 | 0.35 | 0.71 | 1.00 | 1.29 | 1.55 | 1.81 | 2.05 | 2.28 | 2.50 | 2.72 | 2.93 | 3.14 | 3.33 | 3.53 | 3.73 |
| 300 | 0.35 | 0.71 | 1.00 | 1.29 | 1.55 | 1.81 | 2.05 | 2.28 | 2.50 | 2.73 | 2.93 | 3.14 | 3.34 | 3.54 | 3.73 |
| 400 | 0.35 | 0.71 | 1.00 | 1.29 | 1.55 | 1.81 | 2.04 | 2.28 | 2.50 | 2.72 | 2.93 | 3.13 | 3.33 | 3.53 | 3.72 |
| 500 | 0.35 | 0.71 | 1.00 | 1.29 | 1.55 | 1.81 | 2.04 | 2.28 | 2.50 | 2.72 | 2.93 | 3.13 | 3.33 | 3.53 | 3.73 |
| 600 | 0.35 | 0.71 | 1.00 | 1.29 | 1.55 | 1.81 | 2.05 | 2.28 | 2.51 | 2.73 | 2.94 | 3.15 | 3.35 | 3.55 | 3.75 |

TABLE II: Scaling exponents of the longitudinal velocity difference for several Taylor-Scale Reynolds number.

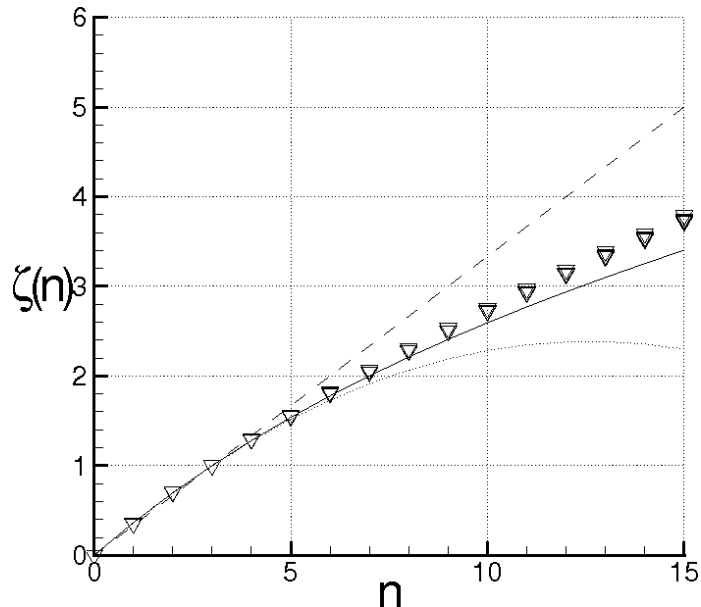


FIG. 9: Scaling exponents of Δu_r for several R . Solid symbols are for the present data. Dashed line is for Kolmogorov K41 data [7]. Dotted line is for Kolmogorov K62 data [8]. Continuous line is for She-Leveque data [9]

where $\langle\langle(\Delta u_r)^n\rangle\rangle$ are calculated with Eqs. (6), \hat{r}_1 is assumed to be equal to 0.1, whereas \hat{r}_2 is taken in such a way that $\zeta(3) = 1$. The so obtained scaling exponents are shown in Table (II) in terms of the Taylor scale Reynolds number, whereas in Fig. 9 (solid symbols) these exponents are compared with those of the Kolmogorov theories K41 [7] (dashed line) and K62 [8] (dotted line), and with the exponents calculated by She-Leveque [9] (continuous curve). Near the origin $\zeta(n) \simeq n/3$, and in general the values of $\zeta(n)$ are in good agreement with the She-Leveque results. In particular the scaling exponents here calculated are lightly greater than those by She-Leveque for $n > 8$.

The PDFs of $\partial u_r / \partial \hat{r}$ are determined by means of Eqs. (9) and (6). Specifically, the PDF is calculated with direct simulations, where the sequences of the variables ξ , η and ζ are first determined by a gaussian random numbers generator. The distribution function is then calculated through the statistical elaboration of the data obtained with Eq. (6). The results are shown in Fig. 10a and 10b in terms of the dimensionless abscissa

$$s = \frac{\partial u_r / \partial \hat{r}}{\langle(\partial u_r / \partial \hat{r})^2\rangle^{1/2}}$$

These distribution functions are normalized, in order that their standard deviations are equal to the unity. The figure represents the PDF for the several R , where the dashed curve

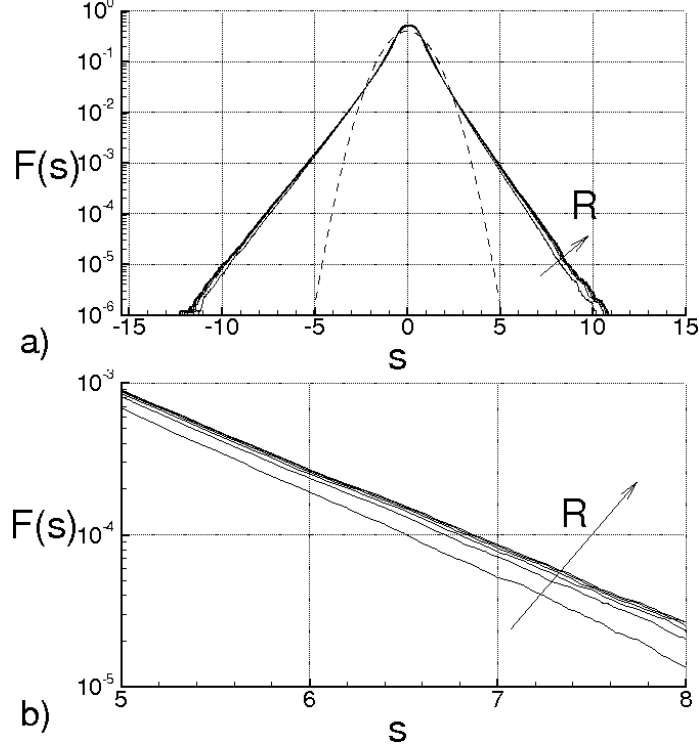


FIG. 10: Probability distribution functions of the longitudinal velocity derivative for the different Taylor-Scale Reynolds numbers

represents the gaussian distribution functions. In particular, Fig. 10b shows the enlarged region of Fig. 10a, where $5 < s < 8$. According to Eq. (6), the tails of PDFs change with R in such a way that the intermittency of $\partial u_r / \partial \hat{r}$ rises with the Reynolds number.

IV. CONCLUSIONS

The obtained self-similar solutions of the von Kármán-Howarth equation with the proposed closure, and the corresponding characteristics of the turbulent flow are shown to be in very good agreement with the various properties of the turbulence from several points of view.

In particular:

- The energy spectrum follows the Kolmogorov law in a range of wave-numbers whose size increases with the Reynolds number.
- The Kolmogorov function exhibits a maximum and relatively small variations in prox-

imity of $r = O(\lambda_T)$. This maximum value rises with the Reynolds number and seems to tend toward the limit $4/5$, prescribed by the Kolmogorov theory.

- The Kolmogorov constant moderately varies with the Reynolds number with an average value around to 1.95 when R varies from 100 to 600.
- The scaling exponents of the moments of velocity difference are calculated through a best fitting procedure in an opportune range of the separation distance. The values of these exponents are in good agreement with the results known from the literature.
- The intermittency of the longitudinal velocity difference rises with the Reynolds number.

These results represent a further test of the analysis presented in Ref. [1] which adequately describes many of the properties of the isotropic turbulence.

V. ACKNOWLEDGMENTS

This work was partially supported by the Italian Ministry for the Universities and Scientific and Technological Research (MIUR).

-
- [1] DE DIVITIIS N., Lyapunov Analysis of Homogeneous Isotropic Turbulence, *arXiv:0905.3513 [physics.flu-dyn]*, 21 May 2009, submitted to Phys. Rev. E.
 - [2] LANDAU, L. D., , LIFSHITZ, M., *Fluid Mechanics*. Pergamon London, England, 1959.
 - [3] VON KÁRMÁN, T. & HOWARTH, L., On the Statistical Theory of Isotropic Turbulence., *Proc. Roy. Soc. A*, **164**, 14, 192, 1938.
 - [4] BATCHELOR G.K., *The Theory of Homogeneous Turbulence*. Cambridge University Press, Cambridge, 1953.
 - [5] VON KÁRMÁN, T. & LIN, C. C., On the Concept of Similarity in the Theory of Isotropic Turbulence., *Reviews of Modern Physics*, **21**, 3, 516, 1949.
 - [6] HILDEBRAND F.B., *Introduction to Numerical Analysis*, Dover Publications, 1987.
 - [7] KOLMOGOROV, A. N., Dissipation of Energy in Locally Isotropic Turbulence. Dokl. Akad. Nauk SSSR **32**, 1, 19–21, 1941.

- [8] KOLMOGOROV, A. N., Refinement of Previous Hypothesis Concerning the Local Structure of Turbulence in a Viscous Incompressible Fluid at High Reynolds Number, *J. Fluid Mech.* **12**, 82–85, 1962.
- [9] SHE Z.S. AND LEVEQUE E., Universal scaling laws in fully developed turbulence, *Phys. Rev. Lett.* **72**, 336, 1994.
- [10] BENZI R., BIFERALE L., PALADIN G., VULPIANI A., VERGASSOLA M., Multifractality in the Statistics of the Velocity Gradients in Turbulence, *Phys. Rev. Lett.* **67**, 2299, 1991.